

See discussions, stats, and author profiles for this publication at: <https://www.researchgate.net/publication/51035643>

Polyaniline-Functionalized Carbon Nanotube Supported Platinum Catalysts

ARTICLE in LANGMUIR · MAY 2011

Impact Factor: 4.46 · DOI: 10.1021/la2003589 · Source: PubMed

CITATIONS

89

READS

92

7 AUTHORS, INCLUDING:



Cheng Xu

China University of Mining Technology

45 PUBLICATIONS 352 CITATIONS

SEE PROFILE



Niancai Cheng

The University of Western Ontario

24 PUBLICATIONS 430 CITATIONS

SEE PROFILE



Huaiguang Li

Ruhr-Universität Bochum

7 PUBLICATIONS 164 CITATIONS

SEE PROFILE



Shichun Mu

Wuhan University of Technology

120 PUBLICATIONS 1,254 CITATIONS

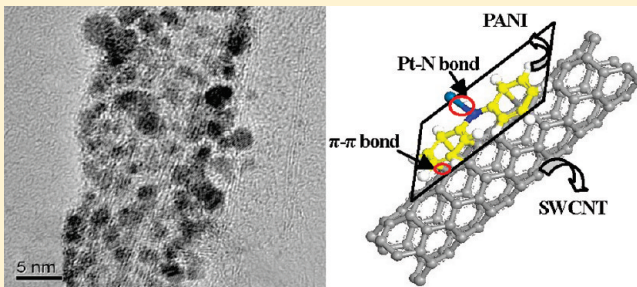
SEE PROFILE

Polyaniline-Functionalized Carbon Nanotube Supported Platinum Catalysts

Daping He,[†] Chao Zeng,[†] Cheng Xu, Niancai Cheng, Huaiguang Li, Shichun Mu,^{*} and Mu Pan

State Key Laboratory of Advanced Technology for Materials Synthesis and Processing, Wuhan University of Technology, Wuhan 430070, People's Republic of China

ABSTRACT: Electrocatalytically active platinum (Pt) nanoparticles on a carbon nanotube (CNT) with enhanced nucleation and stability have been demonstrated through introduction of electron-conducting polyaniline (PANI) to bridge the Pt nanoparticles and CNT walls with the presence of platinum–nitride (Pt–N) bonding and π – π bonding. The Pt colloids were prepared through ethanol reduction under the protection of aniline, the CNT was dispersed well with the existence of aniline in the solution, and aniline was polymerized in the presence of a protonic acid (HCl) and an oxidant ($\text{NH}_4\text{S}_2\text{O}_8$). The synthesized PANI is found to wrap around the CNT as a result of π – π bonding, and highly dispersed Pt nanoparticles are loaded onto the CNT with narrowly distributed particle sizes ranging from 2.0 to 4.0 nm due to the polymer stabilization and existence of Pt–N bonding. The Pt–PANI/CNT catalysts are electroactive and exhibit excellent electrochemical stability and therefore promise potential applications in proton exchange membrane fuel cells.



1. INTRODUCTION

Proton exchange membrane fuel cells (PEMFCs) are receiving widespread attention as a promising power technology for many applications in portable, stationary power sources and automotive engines.^{1,2} However, one of the major challenges for PEMFC commercialization is the production of low-cost electrocatalysts with high catalytic performance and long-term durability under their working conditions. The most commonly used electrocatalysts currently are nanosized platinum (Pt) particles supported on carbon black (CB), usually Vulcan XC72, or XC72 materials. Despite their high surface area and low electrical resistance, low Pt utilization and poor electrochemical stability remain unresolved for Pt/C composite electrocatalysts.^{2–4} Recently, carbon nanotubes (CNTs) have been extensively studied as an alternative catalyst support for PEMFCs, owing primarily to the unique electrical and structural properties of CNTs.^{5,6} Many research groups have reported that the CNT-supported Pt (Pt/CNT) catalysts exhibit increased catalytic activity^{7–9} and show high electrochemical stability^{10,11} compared to Pt/C. However, since the surface of the CNT is highly inert because of high graphitization,^{12,13} Pt nanoparticles are very difficult to deposit directly and evenly onto such surfaces without active functional groups. On the other hand, Pt particles can be readily detached from a support by ultrasonic or/and high-speed agitation treatment during the preparation of catalyst slurries due to low affinity between Pt and carbon atoms. Therefore, how to evenly deposit Pt nanoparticles on the surfaces of CNTs and to reinforce the binding strength between Pt and CNTs become a big challenge. Thus far, the most established protocols for catalytic metal immobilization on CNTs include generating functional groups on the external walls, mostly through harsh oxidative treatment, such as

refluxing in HNO_3 followed by metal deposition on activated CNT walls.^{14–17} Such surface functionalization introduces an avenue for metal precursors to correlate with CNTs and prompts the deposition of metals on the external walls. While these strategies are effective, the full process control has not yet been realized. Other approaches, such as physical evaporation, electronless deposition, and electrodeposition,^{18–23} have also been reported, but satisfactory results are still lacking: the size of the Pt particle on the CNT is difficult to control, dispersion of Pt particles remains uneven, and, most of all, the graphitized surfaces of CNTs are easily destroyed after being eroded by acid treatment, which reduces the conductivity and durability of CNTs. These drawbacks lead to low output performance for Pt/CNT catalysts in PEMFCs.

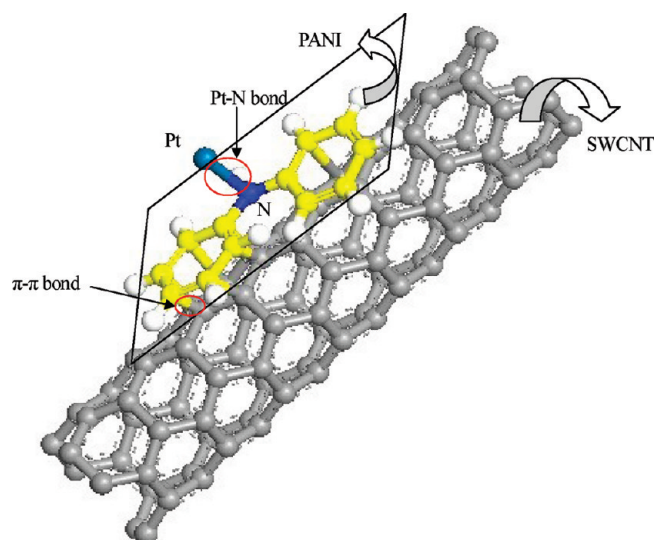
Many of the recent studies on CNTs have focused on their treatment with surfactants, functional polymers, and other capping agents.^{24–28} Evidence shows that such treatment is effective with no breakage on the CNT and enhances the nucleation of Pt nanoparticles onto the inert surfaces of the CNT. In our previous work, we applied perfluorosulfonic acid (PFSA) as a proton conductor to CNT-supported Pt catalysts, and improvement was found in both the dispersion of Pt nanoparticles onto the inert surfaces of CNTs and catalytic performance.²⁹ In the present study, we report a novel approach to the synthesis of Pt/CNT, where electron-conductive polyaniline (PANI) is introduced to bridge Pt nanoparticles and CNTs. It is widely recognized that CNTs consist of sp^2 -hybridized carbon atoms forming a

Received: January 27, 2011

Revised: March 14, 2011

Published: April 08, 2011

Scheme 1. Molecular Interactions in the Synthesized Pt–PANI/CNT Catalyst



hexagonal network, and on the hexagonal network surface there exists a large π -bond. The π -bond interacts with conjugated polymers via π -stacking without disrupting the graphitized surface of the CNT.^{30,31} CNTs modified with conjugated polymers such as PANI have been reported,^{32–35} and Pt particles reportedly adhered strongly to the surfaces of PANI because of the covalent bonding between the Pt atoms and N atoms in PANI. Illustrated in Scheme 1 is a PANI molecule as a cross-linker between Pt nanoparticles and a CNT. The free electron pair of N complexes the space orbital of Pt at the end of the PANI molecule.³⁶ At the other end of the molecule, the phenyl rings connect the backbone of the CNT through π – π bonding. Therefore, the introduction of bridging PANI improves the binding strength between Pt and CNT walls, and PANI possesses the conductivity and high stability as a conductive polymer, properties which are significantly different from those of an aniline monomer;³⁶ it is thus kept after the synthesis of Pt/CNT catalysts to take advantage of these benefits in the current study.

2. EXPERIMENTAL SECTION

All chemicals used in this work were of analytical grade and were used as supplied. High-purity single-walled carbon nanotubes (SWCNTs) were purchased from Shenzhen Nanotech PortCo. Ltd. and used without further treatment. Commercial Pt/C catalyst (20% Pt supported on Vulcan XC-72 carbon) was purchased from JM Co. A 5 wt % Nafion solution was obtained from DuPont.

2.1. Synthesis of Pt–PANI/CNT. SWCNTs, aniline, H_2PtCl_6 (1.5 g/L) aqueous solution, ethanol, and deionized water were mixed and subsequently subjected to mild sonication for 1 h to obtain a highly dispersed aniline-surrounded CNT. The pH of the solution was next adjusted to 8–10 with addition of a NaOH solution, and the solution was refluxed at 130 °C. Pt colloidal nanoparticles were obtained after the solution color changed from yellow to black. Finally the polymerization of aniline was performed with addition of a protonic acid (HCl) and an oxidant ($\text{NH}_4\text{S}_2\text{O}_8$) to give the Pt–PANI/CNT composite with 20% Pt loading. As a reference, 20% Pt/CNT catalysts were prepared using the same method except for the PANI addition.

2.2. Characterization. The morphologies of the prepared catalysts were analyzed with a JEOL 2010 high-resolution transmission electron

microscope. The prepared catalysts were dispersed ultrasonically in ethanol, and an aliquot of this solution was deposited on a grid dried at room temperature. X-ray diffraction (XRD) analysis was performed using a Rigaku X-ray diffractometer with a Cu K α radiation source. The XRD scans were collected at 2 deg min^{–1} from 20° to 90°. The average crystalline size of the Pt nanoparticles was calculated according to the Scherrer equation³⁷ on peak Pt (220):

$$D = \frac{k\lambda}{\beta \cos \theta}$$

where $k = 0.89$, λ (the X-ray wavelength for Cu radiation) = 0.1541 nm, β is the half-height peak width, θ is the Bragg angle corresponding to the peak maximum, and D denotes the average diameter of the crystal pellets. Infrared spectra of the prepared Pt–PANI/CNT catalyst were carried out to detect the presence of PANI in Pt/CNT catalysts with a Fourier transform infrared spectrometer (Nicolet MAGNA-IR 560, FT-IR). The reference PANI was prepared by the same method. X-ray photoelectron spectroscopy (XPS) measurements were performed with a VG Scientific ESCALAB 210 electron spectrometer using Mg KR radiation under a vacuum of 2×10^{-8} Pa.

The electrochemical performance of the catalysts was tested with a three-electrode system. A saturated calomel electrode (SCE) was used as a reference electrode, and platinum wire was used as a counter electrode. The catalysts were added to 500.0 mL of deionized water with 21.0 mL of 5.0 wt % Nafion solution and then dispersed onto the flat surface of a polished glassy carbon disk electrode ($\varphi = 3.0$ mm) as a working electrode using a Finnpiptette digital micropipet (Thermo Electron Corp.) with a catalyst loading of 0.4 mg/cm². The measurements were carried out in 0.5 M H_2SO_4 at a scan rate of 50 mV/s in a potential range of 0–1.2 V vs a normal hydrogen electrode (NHE) at room temperature. The H_2SO_4 solution was saturated with pure argon to expel oxygen out of the solution. The specific electrochemical active area (ECA) was calculated from the following equation:^{38,39}

$$\text{ECA} = \frac{Q_{\text{H}}}{mq_{\text{H}}}$$

where Q_{H} is the charge for H_{upd} adsorption, m is the amount of metal loading, and q_{H} (210 $\mu\text{C}/\text{cm}^2$) is the charge required for monolayer adsorption of hydrogen on Pt surfaces.

Electrochemical accelerated durability tests (ADTs) were employed to evaluate the long-term performance of the catalysts. ADT is an inexpensive and time-effective method for screening catalysts for high stability and good performance.⁴⁰ Using the same system as in a cyclic voltammetry (CV) test, ADT was conducted in the current study with CV curves between 0.6 and 1.20 V.

3. RESULTS AND DISCUSSION

In anticipation of the strong inertness of CNT walls, we prepared the Pt colloidal solution in an aniline and ethanol mixture. As illustrated in Figure 1, besides a polar amino group that can interact with a polar solvent, aniline contains a benzene ring, where aromatic π electrons interact with conjugated π electrons on the CNT surface through π – π interaction. Aniline is therefore regarded as an excellent solvent to wet CNTs, and preparation of Pt colloidal nanoparticles under the protection of aniline also help them to disperse well in the solution. Furthermore, aniline is copolymerized into conductive PANI in the presence of a protonic acid (HCl) and an oxidant ($\text{NH}_4\text{S}_2\text{O}_8$). Thus, PANI brings three advantages at least in this study. First, it is electron conductive as a conductive polymer, so it can transfer electrons from Pt nanoparticles to the CNT. The conductivity and stability of PANI are also greatly enhanced in acidic

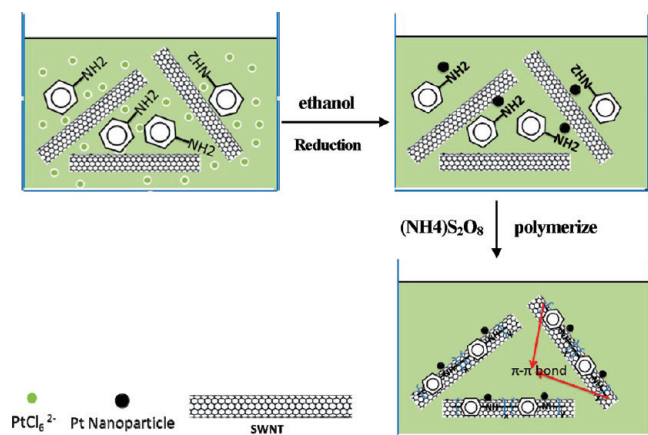


Figure 1. Schematic of the synthetic procedures of Pt–PANI/CNT catalysts.

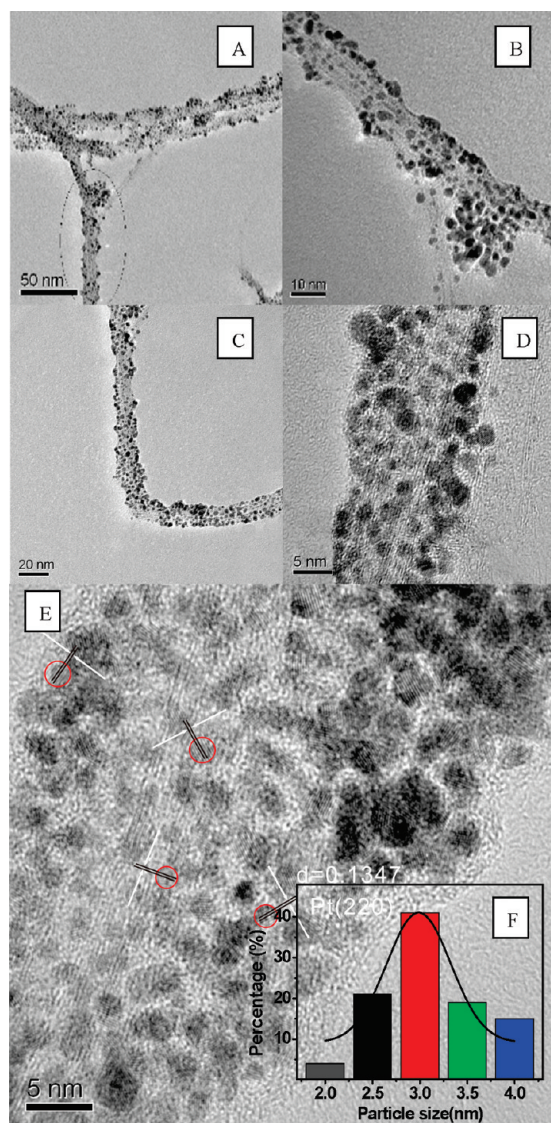


Figure 2. TEM images of 20 wt % Pt–PANI/CNT catalysts (A–D), HRTEM image of the Pt–PANI/CNT catalysts (E), and size distribution of Pt nanoparticles on the CNTs (F).

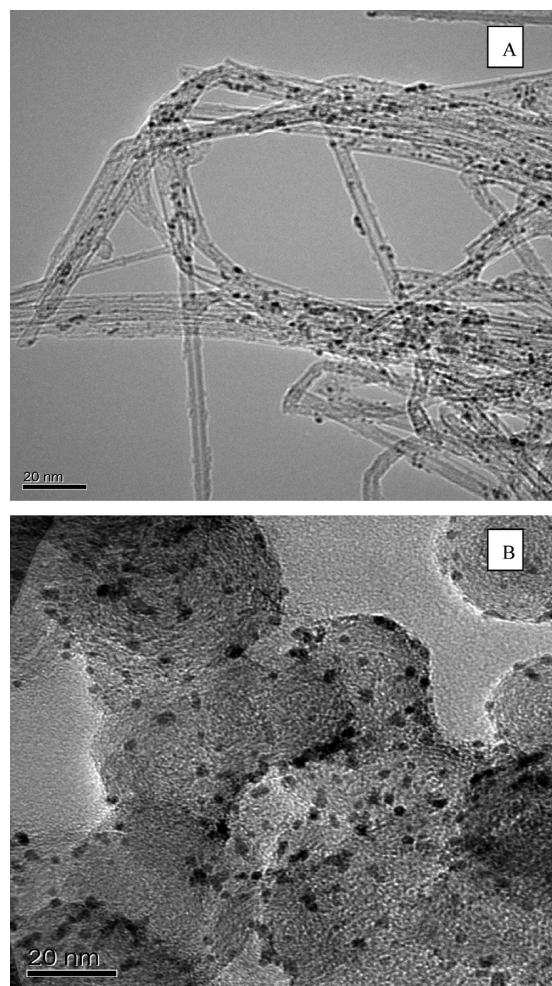


Figure 3. TEM images of 20 wt % Pt/CNT (A) and commercial 20 wt % Pt/C (B) catalysts as a reference.

conditions under which the PEMFC normally operates. Second, it prevents Pt nanoparticles from aggregating with each other through polymeric stabilization and therefore leads to uniform dispersion of Pt nanoparticles on the CNT surfaces.^{29,40–42} Third, Pt nanoparticles can be tightly anchored onto the surfaces of the CNT by forming covalent bonding with the N atoms of PANI as shown in Scheme 1, thus enhancing the catalyst stability.

Figure 2A–D shows that the Pt nanoparticles are well dispersed on the walls of the CNTs in the Pt–PANI/CNT catalysts, and these nanoparticles exhibit no aggregation in larger clusters, but rather form an adlayer-like pattern with uniform particle sizes. Crystalline Pt nanoparticles are found in high-resolution HRTEM micrographs, and the distance between two adjacent lattice planes is approximately 0.135 nm (Figure 2E), which agrees well with the XRD analysis (inset in Figure 2E) and corresponds to Pt(220). Plotted in Figure 2F is the particle size distribution calculated from more than 200 Pt nanoparticles. A really narrow particle size distribution of the Pt nanoparticles is found, with sizes mostly falling between 2.0 and 4.0 nm. Apparently a large amount of external amino groups in PANI on the surfaces of the CNTs helps increase the loading and preserve the dispersion of Pt nanoparticles. By contrast a lower dispersion of Pt nanoparticles on the walls of the nanotubes is presented in the Pt/CNT catalysts (Figure 3A), indicating an ununiform distribution of Pt nanoparticles on the support surfaces

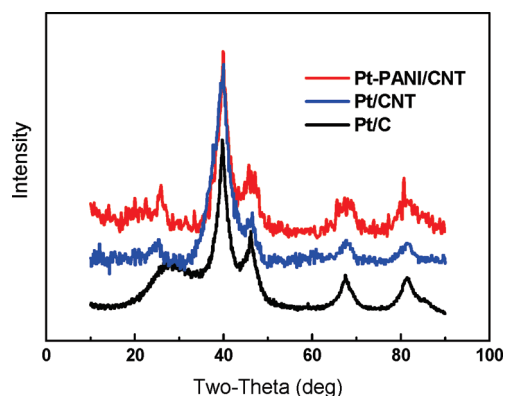


Figure 4. XRD patterns of Pt–PANI/CNT, Pt/CNT, and Pt/C catalysts.

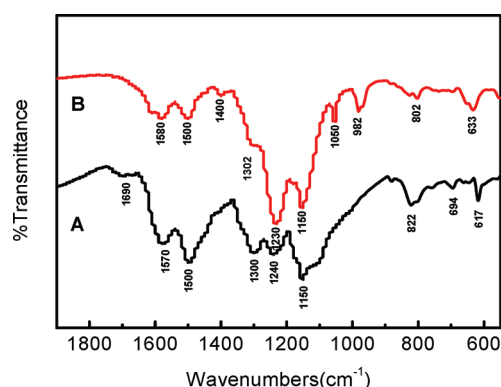


Figure 5. FT-IR spectra of PANI (A) and Pt–PANI/CNT (B) catalysts.

without PANI functionalization. The commercial Pt/C catalysts as a reference have a Pt particle size comparable with that of the Pt–PANI/CNT catalysts (Figure 3B).

The XRD patterns of the Pt–PANI/CNT, Pt/CNT, and Pt/C catalysts are revealed in Figure 4. The peaks between 20° and 90° can be indexed to Pt crystals of face-centered cubic (fcc) structure. The peaks at $2\theta = 39.70^\circ$, 46.46° , 67.70° , and 81.42° are assigned to the (111), (200), (220), and (311) planes of Pt, respectively. The average crystalline sizes of Pt for Pt–PANI/CNT, Pt/CNT, and Pt/C were 3.1, 3.3, and 3.4 nm, respectively.

FT-IR spectra of the PANI and Pt–PANI/CNT catalysts are presented in Figure 5. For the Pt–PANI/CNT catalysts, two characteristic bands at 1230 and 1302 cm^{-1} can be assigned to C=N and C–N stretching vibrations, corresponding to the bands at 1240 and 1300 cm^{-1} in PANI. The peak at 1570 cm^{-1} is associated with quinoid ring vibration, while the band at 1500 cm^{-1} is from benzene ring vibration, corresponding to the bands at 1580 and 1500 cm^{-1} in PANI, respectively. A characteristic conductivity peak of PANI, the strong band at 1150 cm^{-1} was described by MacDiarmid et al. as an “electronic-like band” and is considered to be a measure of the degree of delocalization of electrons.^{43,44} These results also verify the presence of PANI in the as-prepared Pt/CNT catalysts.

Shown in Figure 6A are the XPS spectra of Pt–PANI/CNT and Pt/CNT. Besides the C(1s) signal at 284.2 eV and the O(1s) signal at 543.1 eV, the Pt(4f), Pt(5s), Pt(4p), and Pt(4d) signals appear in both samples.^{25,45} It is noteworthy that the N(1s) signal originating from PANI is observed only in the Pt–PANI/CNT

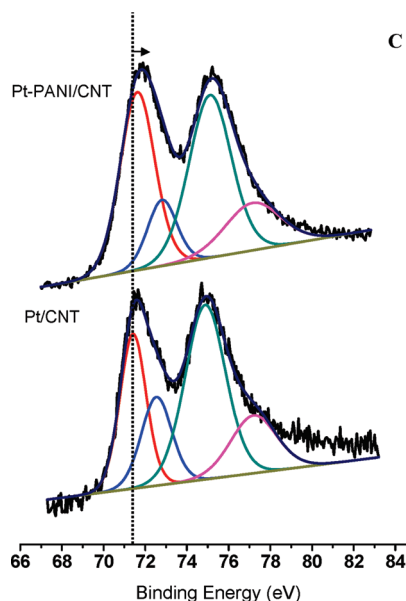
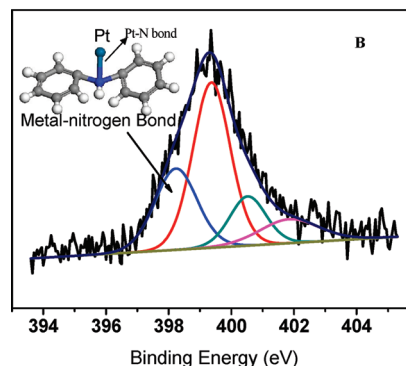
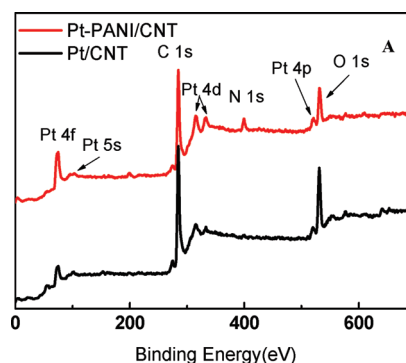


Figure 6. XPS spectra of Pt–PANI/CNT and Pt/CNT catalysts (A), XPS spectra of N(1s) bonds (B), and XPS spectra of the Pt(4f) bands (C).

but not in the Pt/CNT samples. As shown in Figure 6B, the N(1s) line was deconvoluted into four superimposed peaks at 398.23, 399.37, 400.53, and 401.85 eV. The peaks at 399.37 and 400.53 eV are characteristic peaks for the amine-like nitrogen atoms (–NH–) and the cationic nitrogen atoms on the polymer backbone compensated with counterions (SO_4^{2-}), respectively. The highest binding energy (401.85 eV) peak is due to the protonated amine units.^{46,47} The peak at 398.23 eV demonstrates the presence of platinum–nitride bonding between the N atoms of PANI and the surface Pt atoms of the Pt nanoparticles.^{24,25,48} These spectral

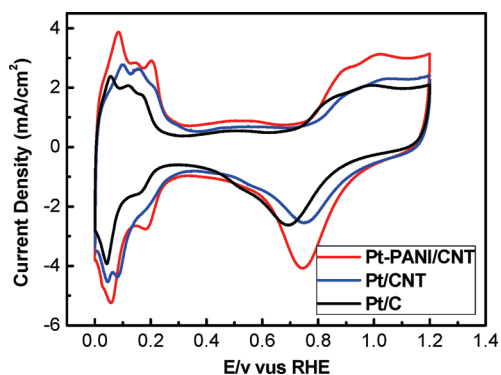


Figure 7. CV curves of Pt–PANI/CNT, Pt/CNT, and Pt/C catalysts.

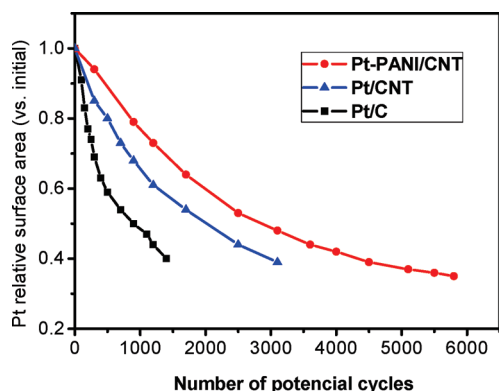


Figure 8. ECA of the catalysts as a function of the number of potential cycles.

results illustrate the bifunctional stabilizing mechanism of PANI on Pt particles. The Pt(4f) line in Figure 6C shows two pairs of peaks from the spin–orbital splitting of the $4f_{7/2}$ and $4f_{5/2}$ regions due to metallic Pt (71.7 eV) and oxide species (74.8 eV), respectively.⁴⁹ The two catalysts show essentially identical ratios of metallic Pt to oxide species, and no significant differences are observed in the abundance ratio. However, a shift to higher energy is found in the binding energies of the PANI-functionalized CNT-supported Pt. The slight shift of the Pt peak toward higher binding energies is due likely to the presence of Pt–N bonding and the effect of small particles in the Pt–PANI/CNT catalysts.⁵⁰

Figure 7 presents CV curves of Pt–PANI/CNT, Pt/CNT, and Pt/C catalysts recorded at room temperature. The ECA is calculated from measuring the charges collected in the hydrogen adsorption/desorption region after double-layer correction and assuming a value of $210 \mu\text{C cm}^{-2}$ for the adsorption of a hydrogen monolayer.^{37,38} Significantly, Pt–PANI/CNT gives a higher ECA ($64.5 \text{ m}^2 \text{ g}^{-1}$) than both the Pt/CNT ($58.4 \text{ m}^2 \text{ g}^{-1}$) and Pt/C ($50.2 \text{ m}^2 \text{ g}^{-1}$) catalysts. The ECA increases by 28% compared to that of Pt/C. The increase of ECA should derive from the optimized dispersion and size distribution of Pt nanoparticles through use of polar aniline as a dispersant and the polymeric stabilization mechanism of PANI.

The ECA loss of Pt over different electrochemical oxidation cycles is shown in Figure 8. The ECA losses of all catalysts decrease with an increase in the number of cycles under the same electrochemical acceleration test. According to the correlations, the durability of Pt/C is much lower than that of Pt/CNT in this work. ECA drops to 40% of the initial value after Pt/C experiences

1400 cycles or Pt/CNT 3100 cycles, indicating that Pt–PANI/CNT has higher stability than Pt/CNT. Pt–PANI/CNT experiences 4500 cycles before ECA drops to 40% of the initial value, and it remains at 38% after 5800 cycles. Such findings clearly demonstrate that our prepared Pt–PANI/CNT has an electrochemical durability 3 times longer than that of Pt/C and 1.5 times longer than that of plain Pt/CNT with 40% as the benchmark under the same ADT conditions. The greatly improved durability can be caused by the bridging position of PANI between Pt nanoparticles and CNT walls with the presence of platinum–nitride bonding and π – π bonding and the polymeric stabilization of PANI, which can effectively prevent the Pt nanoparticles from aggregating with each other and motion and thus mitigate aggregation of Pt nanoparticles.

4. CONCLUSION

A new method to synthesize Pt/CNT catalysts with PANI to bridge Pt and CNTs has been successfully developed. Monodispersed Pt nanoparticles with a very narrow particle size distribution ranging between 2.0 and 4.0 nm can be anchored onto the surface of PANI not only because the free electron pair of N interacts with the space orbital of Pt to form a coordination complex, but also because PANI containing aromatic groups links to carbon atomic sheets of CNTs through π – π bonding. The existence of Pt has shown no influence on the π – π bonding between PANI and CNTs, while aniline polymerizes completely. Cyclic voltammetry and ADT tests show our novel Pt/CNT catalysts are electroactive and exhibit excellent electrochemical stability that promises potential applications in PEMFCs and other uses.

AUTHOR INFORMATION

Corresponding Author

*Fax: +86 27 87879468. E-mail: msc@whut.edu.cn.

Author Contributions

[†]These authors contributed equally to this work.

ACKNOWLEDGMENT

This work was supported by the National Natural Science Foundation of China (NSFC; Grants 50972112 and 50632050) and the Fundamental Research Funds for the Central Universities.

REFERENCES

- (1) Wee, J.-H. Applications of proton exchange membrane fuel cell systems. *Renewable Sustainable Energy Rev.* **2007**, *11* (8), 1720–1738.
- (2) Saha, M. S.; Li, R.; Sun, X.; Ye, S. 3-D composite electrodes for high performance PEM fuel cells composed of Pt supported on nitrogen-doped carbon nanotubes grown on carbon paper. *Electrochem. Commun.* **2009**, *11* (2), 438–441.
- (3) Stevens, D. A.; Dahn, J. R. Thermal degradation of the support in carbon-supported platinum electrocatalysts for PEM fuel cells. *Carbon* **2005**, *43* (1), 179–188.
- (4) Gasteiger, H. A.; Kocha, S. S.; Sompalli, B.; Wagner, F. T. Activity benchmarks and requirements for Pt, Pt-alloy, and non-Pt oxygen reduction catalysts for PEMFCs. *Appl. Catal., B* **2005**, *56* (1–2), 9–35.
- (5) Kongkanand, A.; Kuwabata, S.; Girishkumar, G.; Kamat, P. Single-wall carbon nanotubes supported platinum nanoparticles with improved electrocatalytic activity for oxygen reduction reaction. *Langmuir* **2006**, *22* (5), 2392–2396.
- (6) Wang, D.; Lu, S.; Jiang, S. P. Tetrahydrofuran-functionalized multi-walled carbon nanotubes as effective support for Pt and PtSn electrocatalysts of fuel cells. *Electrochim. Acta* **2010**, *55* (8), 2964–2971.

- (7) Li, W.; Liang, C.; Zhou, W.; Qiu, J.; Zhou, S.; Sun, G.; Xin, Q. Preparation and characterization of multiwalled carbon nanotube-supported platinum for cathode catalysts of direct methanol fuel cells. *J. Phys. Chem. B* **2003**, *107* (26), 6292–6299.
- (8) Wu, G.; Chen, Y.-S.; Xu, B.-Q. Remarkable support effect of SWNTs in Pt catalyst for methanol electrooxidation. *Electrochem. Commun.* **2005**, *7* (12), 1237–1243.
- (9) Che, G.; Lakshmi, B. B.; Martin, C. R.; Fisher, E. R. Metal-nanocluster-filled carbon nanotubes: Catalytic properties and possible applications in electrochemical energy storage and production. *Langmuir* **1999**, *15* (3), 750–758.
- (10) Shao, Y.; Yin, G.; Gao, Y.; Shi, P. Durability study of Pt/C and Pt/CNTs catalysts under simulated PEM fuel cell conditions. *J. Electrochem. Soc.* **2006**, *153* (6), A1093–A1097.
- (11) Wang, X.; Li, W.; Chen, Z.; Waje, M.; Yan, Y. Durability investigation of carbon nanotube as catalyst support for proton exchange membrane fuel cell. *J. Power Sources* **2006**, *158* (1), 154–159.
- (12) Soin, N.; Roy, S. S.; Karlsson, L.; McLaughlin, J. A. Sputter deposition of highly dispersed platinum nanoparticles on carbon nanotube arrays for fuel cell electrode material. *Diamond Relat. Mater.* **2010**, *19* (5–6), 595–598.
- (13) Sun, X.; Li, R.; Villers, D.; Dodelet, J. P.; Désilets, S. Composite electrodes made of Pt nanoparticles deposited on carbon nanotubes grown on fuel cell backings. *Chem. Phys. Lett.* **2003**, *379* (1–2), 99–104.
- (14) Yu, R.; Chen, L.; Liu, Q.; Lin, J.; Tan, K.-L.; Ng, S. C.; Chan, H. S. O.; Xu, G.-Q.; Hor, T. S. A. Platinum deposition on carbon nanotubes via chemical modification. *Chem. Mater.* **1998**, *10* (3), 718–722.
- (15) Hirsch, A. Functionalization of single-walled carbon nanotubes. *Angew. Chem., Int. Ed.* **2002**, *41* (11), 1853–1859.
- (16) Tian, Z. Q.; Jiang, S. P.; Liang, Y. M.; Shen, P. K. Synthesis and characterization of platinum catalysts on multiwalled carbon nanotubes by intermittent microwave irradiation for fuel cell applications. *J. Phys. Chem. B* **2006**, *110* (11), 5343–5350.
- (17) Liang, Y.; Zhang, H.; Yi, B.; Zhang, Z.; Tan, Z. Preparation and characterization of multi-walled carbon nanotubes supported PtRu catalysts for proton exchange membrane fuel cells. *Carbon* **2005**, *43* (15), 3144–3152.
- (18) Kong, J.; Chapline, M. G.; Dai, H. Functionalized carbon nanotubes for molecular hydrogen sensors. *Adv. Mater.* **2001**, *13* (18), 1384–1386.
- (19) Bezryadin, A.; Lau, C. N.; Tinkham, M. Quantum suppression of superconductivity in ultrathin nanowires. *Nature* **2000**, *404* (6781), 971–974.
- (20) Choi, H. C.; Shim, M.; Bangsaruntip, S.; Dai, H. Spontaneous reduction of metal ions on the sidewalls of carbon nanotubes. *J. Am. Chem. Soc.* **2002**, *124* (31), 9058–9059.
- (21) Girishkumar, G.; Vinodgopal, K.; Kamat, P. V. Carbon nanostructures in portable fuel cells: single-walled carbon nanotube electrodes for methanol oxidation and oxygen reduction. *J. Phys. Chem. B* **2004**, *108* (52), 19960–19966.
- (22) Tang, Z.; Ng, H. Y.; Lin, J.; Wee, A. T. S.; Chua, D. H. C. Pt/CNT-based electrodes with high electrochemical activity and stability for proton exchange membrane fuel cells. *J. Electrochem. Soc.* **2010**, *157* (2), B245–B250.
- (23) Quinn, B. M.; Dekker, C.; Lemay, S. G. Electrodeposition of noble metal nanoparticles on carbon nanotubes. *J. Am. Chem. Soc.* **2005**, *127* (17), 6146–6147.
- (24) Wang, S.; Wang, X.; Jiang, S. P. PtRu nanoparticles supported on 1-aminopyrene-functionalized multiwalled carbon nanotubes and their electrocatalytic activity for methanol oxidation. *Langmuir* **2008**, *24* (18), 10505–10512.
- (25) Hsin, Y. L.; Hwang, K. C.; Yeh, C.-T. Poly(vinylpyrrolidone)-modified graphite carbon nanofibers as promising supports for PtRu catalysts in direct methanol fuel cells. *J. Am. Chem. Soc.* **2007**, *129* (32), 9999–10010.
- (26) Ding, W.; Eitan, A.; Fisher, F. T.; Chen, X.; Dikin, D. A.; Andrews, R.; Brinson, L. C.; Schadler, L. S.; Ruoff, R. S. Direct observation of polymer sheathing in carbon nanotube-polycarbonate composites. *Nano Lett.* **2003**, *3* (11), 1593–1597.
- (27) Mu, Y.; Liang, H.; Hu, J.; Jiang, L.; Wan, L. Controllable Pt nanoparticle deposition on carbon nanotubes as an anode catalyst for direct methanol fuel cells. *J. Phys. Chem. B* **2005**, *109* (47), 22212–22216.
- (28) Yang, D. Q.; Hennequin, B.; Sacher, E. XPS demonstration of π - π interaction between benzyl mercaptan and multiwalled carbon nanotubes and their use in the adhesion of Pt nanoparticles. *Chem. Mater.* **2006**, *18* (21), 5033–5038.
- (29) He, D.; Mu, S.; Pan, M. Perfluorosulfonic acid-functionalized Pt/carbon nanotube catalysts with enhanced stability and performance for use in proton exchange membrane fuel cells. *Carbon* **2011**, *49* (1), 82–88.
- (30) Yang, D.-Q.; Rochette, J.-F.; Sacher, E. Spectroscopic evidence for π - π interaction between poly(diallyl dimethylammonium) chloride and multiwalled carbon nanotubes. *J. Phys. Chem. B* **2005**, *109* (10), 4481–4484.
- (31) Chen, R. J.; Zhang, Y.; Wang, D.; Dai, H. Noncovalent sidewall functionalization of single-walled carbon nanotubes for protein immobilization. *J. Am. Chem. Soc.* **2001**, *123* (16), 3838–3839.
- (32) Bauhofer, W.; Kovacs, J. Z. A review and analysis of electrical percolation in carbon nanotube polymer composites. *Compos. Sci. Technol.* **2009**, *69* (10), 1486–1498.
- (33) Zhou, Y.-k.; He, B.-l.; Zhou, W.-j.; Huang, J.; Li, X.-h.; Wu, B.; Li, H.-l. Electrochemical capacitance of well-coated single-walled carbon nanotube with polyaniline composites. *Electrochim. Acta* **2004**, *49* (2), 257–262.
- (34) O'Connell, M. J.; Boul, P.; Ericson, L. M.; Huffman, C.; Wang, Y.; Haroz, E.; Kuper, C.; Tour, J.; Ausman, K. D.; Smalley, R. E. Reversible water-solubilization of single-walled carbon nanotubes by polymer wrapping. *Chem. Phys. Lett.* **2001**, *342* (3–4), 265–271.
- (35) Guo, L.; Peng, Z. One-pot synthesis of carbon nanotube-polyaniline-gold nanoparticle and carbon nanotube-gold nanoparticle composites by using aromatic amine chemistry. *Langmuir* **2008**, *24* (16), 8971–8975.
- (36) Hsu, C.-H.; Liao, H.-Y.; Kuo, P.-L. Aniline as a dispersant and stabilizer for the preparation of Pt nanoparticles deposited on carbon nanotubes. *J. Phys. Chem. C* **2010**, *114* (17), 7933–7939.
- (37) Radmilovic, V.; Gasteiger, H. A.; Ross, P. N. Structure and chemical composition of a supported Pt-Ru electrocatalyst for methanol oxidation. *J. Catal.* **1995**, *154* (1), 98–106.
- (38) Schmidt, T. J.; Gasteiger, H. A.; Stab, G. D.; Urban, P. M.; Kolb, D. M.; Behm, R. J. Characterization of high-surface-area electrocatalysts using a rotating disk electrode configuration. *J. Electrochem. Soc.* **1998**, *145* (7), 2354–2358.
- (39) Colombi Ciacchi, L.; Pompe, W.; De Vita, A. Growth of platinum clusters via addition of Pt(II) complexes: A first principles investigation. *J. Phys. Chem. B* **2003**, *107* (8), 1755–1764.
- (40) Cheng, N.; Mu, S.; Pan, M.; Edwards, P. P. Improved lifetime of PEM fuel cell catalysts through polymer stabilization. *Electrochem. Commun.* **2009**, *11* (8), 1610–1614.
- (41) Cheng, N.; Lv, H.; Wang, W.; Mu, S.; Pan, M.; Marken, F. An ambient aqueous synthesis for highly dispersed and active Pd/C catalyst for formic acid electro-oxidation. *J. Power Sources* **2010**, *195* (21), 7246–7249.
- (42) Yin, S.; Mu, S.; Lv, H.; Cheng, N.; Pan, M.; Fu, Z. A highly stable catalyst for PEM fuel cell based on durable titanium diboride support and polymer stabilization. *Appl. Catal., B* **2010**, *93* (3–4), 233–240.
- (43) Zengin, H.; Zhou, W.; Jin, J.; Czerw, R.; Smith, D. W.; Echegoyen, L.; Carroll, D. L.; Foulger, S. H.; Ballato, J. Carbon nanotube doped polyaniline. *Adv. Mater.* **2002**, *14* (20), 1480–1483.
- (44) Quillard, S.; Louarn, G.; Lefrant, S.; Macdiarmid, A. G. Vibrational analysis of polyaniline: A comparative study of leucoemeraldine, emeraldine, and pernigraniline bases. *Phys. Rev. B* **1994**, *50* (17), 12496.
- (45) Liu, Z.; Lee, J. Y.; Chen, W.; Han, M.; Gan, L. M. Physical and electrochemical characterizations of microwave-assisted polyol preparation of carbon-supported PtRu nanoparticles. *Langmuir* **2003**, *20* (1), 181–187.
- (46) Wu, G.; Li, L.; Li, J.-H.; Xu, B.-Q. Polyaniline-carbon composite films as supports of Pt and PtRu particles for methanol electrooxidation. *Carbon* **2005**, *43* (12), 2579–2587.
- (47) Zhou, Y.-k.; He, B.-l.; Zhou, W.-j.; Li, H.-l. Preparation and electrochemistry of SWNT/PANI composite films for electrochemical capacitors. *J. Electrochem. Soc.* **2004**, *151* (7), A1052–A1057.

- (48) Kuo, P.-L.; Chen, W.-F.; Huang, H.-Y.; Chang, I. C.; Dai, S. A. Stabilizing effect of pseudo-dendritic polyethylenimine on platinum nanoparticles supported on carbon. *J. Phys. Chem. B* **2006**, *110* (7), 3071–3077.
- (49) Onoe, T.; Iwamoto, S.; Inoue, M. Synthesis and activity of the Pt catalyst supported on CNT. *Catal. Commun.* **2007**, *8* (4), 701–706.
- (50) Roth, C.; Goetz, M.; Fuess, H. Synthesis and characterization of carbon-supported Pt–Ru–WO_x catalysts by spectroscopic and diffraction methods. *J. Appl. Electrochem.* **2001**, *31* (7), 793–798.